Journal of Data Science and Modeling, Vol. 3, No. 2, 115-136, June 2025

Research Manuscript

Predicting Temperament and Cardiac Strength from Persian Medicine Pulsology Using Artificial Neural Networks

Mohammad Dehghandar*[1], Mahdi Alizadeh Vaghasloo†[2,3], Ghasem Ahmadi[1]

m_dehghandar@pnu.ac.ir, mhdalizadeh@gmail.com, g.ahmadi@pnu.ac.ir

[1]Department of Mathematics, Payame Noor University, Tehran, Iran.

[2]Department of Traditional Medicine, School of Persian Medicine, Tehran University of Medical Sciences, Tehran, Iran

[3]Persian Medicine Network (PMN), Universal Scientific Education and Research Network (USERN), Tehran, Iran

Recieved: 10/02/2026 Accepted: 30/08/2026

Abstract:

Persian Medicine (PM) pulsology is a central diagnostic modality for assessing an individual's temperamental state and cardiac strength; however, its practical application is inherently subjective and dependent on practitioner expertise. To enhance objectivity and reproducibility in PM diagnostics, this study proposes an artificial neural network (ANN) framework for the quantitative estimation of four core temperamental qualities—warmness, coldness, wetness, and dryness—together with cardiac strength, based solely on measurable pulse characteristics. Clinical data were collected from 69 individuals, comprising 11 pulse-derived features and gender as inputs, with six corresponding diagnostic outputs. A multilayer perceptron (MLP) architecture was trained and optimized using two learning algorithms: Levenberg–Marquardt (LM) and Scaled Conjugate Gradient (SCG). Comparative evaluation demonstrated the superiority of the SCG-trained network, with an optimal configuration of 12 hidden neurons. This model achieved a test accuracy of 96.43% and a low mean squared error (MSE) of 0.0139. Notably, cardiac strength was predicted with 100% accuracy, while temperamental qualities

*Corresponding Author: m_dehghandar@pnu.ac.ir

†Corresponding Author: mhdalizadeh@gmail.com

were classified with accuracies ranging from 71.43% to 92.86%. To enhance interpretability, a sensitivity analysis was conducted, revealing pulse strength and pulse frequency as the most influential predictors across multiple diagnostic outputs. The proposed ANN-based system provides a stable and objective computational surrogate for traditional PM pulsology. It offers practical utility for practitioner training, supports diagnostic standardization, and establishes a methodological foundation for future integrative and intelligent diagnostic platforms in Persian Medicine.

Keywords: Persian medicine (PM), artificial neural network (ANN), pulse diagnosis, temperamental, scaled conjugate gradient (SCG).
Mathematics Subject Classification (2010): 92C40, 62H30.

1. Introduction

The global trajectory of medicine is increasingly oriented toward an integrative model that synergistically combines the advantages of traditional and complementary medical systems with conventional healthcare (World Health Organization , 2014). Persian Medicine (PM) represents one of the most comprehensive and historically grounded schools of traditional medicine, with centuries of documented practice across vast geographical regions (Rezaeizadeh et al. , 2009; Sharifi Darani et al. , 2021). PM is widely recognized as a comprehensive and historically rich traditional medical system, with centuries of documented practice across diverse geographical regions Pirooz et al. (2026).

Persian Medicine (PM) classifies individuals into fundamental temperamental categories, known as *Mizaj*, based on the phenotypic manifestations of warmth, coldness, wetness, and dryness (Shirbeigi et al. , 2017). It is critical to note that these qualities represent a holistic, systemic metabolic profile shaped by diverse physiological and environmental factors, not merely physical body temperature (Shirbeigi et al. , 2017). Contemporary scientific investigations have provided growing empirical support for these temperamental distinctions Alizadeh et al. (2025). A growing body of contemporary research provides empirical support for these categorical distinctions (Rezadoost et al. , 2016). Accurately assessing a person's *Mizaj*, along with cardiac strength and overall vitality, is therefore a cornerstone of PM for formulating personalized health strategies and therapeutic interventions. Clinicians deduce these qualities from a constellation of clinical signs, among which the diagnosis of the pulse holds exceptional importance. Indeed, pulsology constitutes more than a quarter of all diagnostic material in classical PM texts, highlighting its central clinical role (Alizadeh et al. , 2012). This positions pulse analysis as a highly promising avenue for improving disease identification and management within the PM framework. Each pulse is described by a set of distinct parameters—such as its spatial dimensions, rhythm, force, and thermal properties—which together offer a composite window into systemic health and organ function (Dehghandar et al. , 2016; Vaghasloo , 2013).

Despite its diagnostic value, pulse assessment in PM heavily relies on practitioner expertise and experiential knowledge, which poses challenges for standardization and training (Dehghandar , 2016; Alizadeh et al. , 2025). Recent advances in computational medicine have highlighted the role of intelligent systems—particularly AI and neural networks—in integrating traditional diagnostic methods with modern technologies, opening new avenues for innovation in PM research (Nafisi , 2017; Dehghandar et al. , 2026, 2024). This study employs AI and neural network modeling to replicate the pulse-based diagnostic reasoning of PM experts in determining temperament and physiological strength. The following sections elaborate on the foundational concepts of pulse theory and neural networks, introduce the confusion matrix as an evaluative framework, and detail the dataset and ANN architecture implemented.

1.1 Pulse in Persian Medicine

In both PM literature and modern physiology, the pulse is defined as the rhythmic expansion of an artery resulting from cardiac ejection of blood into the arterial system. Each pulsation consists of two phases—expansion and contraction—separated by brief intervals. Within PM, the pulse is regarded as one of the most reliable indicators of systemic health and disease, as well as the optimal metric for evaluating cardiac function. Pulse examination is typically conducted at the radial artery under strictly controlled conditions, including ambient thermal comfort, physical and mental repose, and focused attention from both examiner and patient. The examiner must carefully regulate finger placement, orientation, angle, and applied pressure, as these factors significantly influence pulse perception and interpretation (Naseri et al. , 2010).

PM recognizes multiple pulse parameters that convey information about bodily states and vital organ function. Key parameters referenced in this study include (Chashti , 2008; Alizadeh et al. , 2017):

- Pulse length, width, and height: The spatial dimensions of the pulse wave.
- Pulse strength, speed, and frequency: The force, temporal duration, and recurrence rate of the pulse.
- Vascular fullness and consistency: The sense of vessel repletion and arterial wall pliability.
- Thermal parameters: Including palmar, dorsal hand, and arterial temperatures.

Although a talented PM practitioner may deduce the patient's temperament and heart strength from an overall assessment of these parameters, it is often difficult for students or less experienced practitioners to do so correctly and consistently.

1.2 Artificial Neural Network (ANN)

An artificial neural network (ANN) is a non-parametric computational model capable of classifying subjects or estimating outcomes based on a set of input variables (Baldi et al. , 2025; Mellina Andreu et al. , 2025; Chierici et al. , 2025;

?). Drawing inspiration from biological neural networks, ANNs are particularly well-suited for capturing complex, nonlinear relationships within data (Mouazen et al. , 2025). A widely adopted structure is the multilayer perceptron (MLP), which typically outperforms simpler models across various tasks. The MLP comprises an input layer, one or more hidden layers, and an output layer. ANNs learn from data through a process of supervised training, where the error between the network output and the target is minimized using optimization algorithms such as backpropagation (Ramón-Fernández et al. , 2020; Li et al. , 2025). Various training algorithms are available; in this study, the Levenberg–Marquardt (LM) and Scaled Conjugate Gradient (SCG) algorithms were employed and compared for efficiency and convergence.

1.3 Study Aim and Objectives

Given the clinical significance and interpretative challenges of PM pulsology, this study aimed to design and optimize an ANN to estimate the continuous values of warmness, coldness, wetness, dryness, and cardiac strength from a standardized set of pulse parameters. The specific objectives were to:

- Systematically compare the performance of LM and SCG training algorithms across different architectural complexities.
- Identify the optimal network configuration based on regression accuracy and stability.
- Evaluate the model's performance using appropriate statistical and clinical metrics.
- Interpret the model via sensitivity analysis to identify the most influential pulse parameters, thereby linking computational results to PM diagnostic principles.

2. Materials and Methods

2.1 Data Source and Preprocessing

Clinical data were obtained from 69 subjects (37 male, 32 female) examined at the Traditional Persian Medicine Clinic of Tehran University of Medical Sciences. A specialist recorded twelve input variables: eleven pulse parameters (eight ordinal on a 1–3 scale, three continuous temperatures) and gender (binary). Six target variables were determined by the specialist: Warmness #1 (count-based), Warmness #2 (intensity-based), Coldness, Wetness, Dryness, and Cardiac Strength.

Also, the PM physician helped to score warmness #1 and #2, coldness, wetness, dryness, and strength between 0 and 13 using the pulse rules. To assess which kind of score summation is more correlated with the input parameters, two methods of summation were considered as a sample for warmness, which is the quality most related to vital power. The first is named simply as the degree of warmness #1, being calculated from the sum of the number of parameters indicating warmness, and the second is named as the degree of warmness #2, being calculated from the total summation of the score of parameters indicating warmness. For example, a person with pulse parameters of Speed = 2, Frequency = 3, Strength = 3, Length = 1, and Height = 2 (all indicating warmth) has a total intensity-based Warmness #2 score of 11, while the same individual was clinically assessed by the PM specialist as having a Warmness #1 degree of 2 (count-based). All variables were normalized to [0, 1] using min-max scaling. Table 1 shows the general status of input and output data for ANN design. These data are speed, frequency, strength, length, height, wetness, vascular fullness, width, temperature of palms, temperature of backhand, artery's temperature, gender (Male: 37, Female: 32), degree of warmness #1, warmness #2, coldness, wetness, dryness, and strength.

Table 1: Data status for the ANN designed to estimate warmness, coldness, wetness, dryness, and strength.

I/O	Variables	Min	Max	Mean
I_1	Pulse Speed	1	3	1.8750
I_2	Pulse Frequency	1	3	2.1250
I_3	Pulse Strength	0	3	2.1786
I_4	Pulse Length	1	3	1.2143
I_5	Pulse Height	1	3	2.1875
I_6	Pulse Wetness	1	3	2.2500
I_7	Pulse Vascular fullness	1	3	2.4196
I_8	Pulse Width	1	3	2.1964
I_9	Temperature of palms	34	38	36.2500
I_{10}	Temperature of backhand	34	37.5	35.1161
I_{11}	Artery's temperature	34	38	35.8348
I_{12}	Gender (Male: 37, Female: 32)	-	-	-
O_1	Warmness #1	0	4	0.8214
O_2	Warmness #2	6	13	9.5804
O_3	Coldness	0	4	1.1964
O_4	Wetness	0	3	1.4643
O_5	Dryness	0	3	0.5714
O_6	Strength	0	2	0.4107

2.2 Data Partitioning and Validation Strategy

The dataset ($n = 69$) was randomly split into a training set ($n = 55$, $\sim$80%) and a hold-out test set ($n = 14$, $\sim$20%). To implement early stopping and prevent overfitting, the training set was further subdivided using a hold-out method within the training phase: 45 samples ($\sim$65% of total data) for parameter optimization and 10 samples ($\sim$15% of total data) as a dedicated validation set to monitor generalization error during training. The final model, selected based on the lowest validation error, was then evaluated once on the completely independent test set ($n = 14$) to report its true generalization performance (e.g., Test MSE = 0.0139, Test Accuracy = 96.4% for the optimal SCG-12 model). Due to the limited sample size, a single random split was utilized. To account for the stochasticity of weight initialization, each architectural configuration was trained 10 times with different random seeds, and the performance metrics are presented as the mean $\pm$ standard deviation across these runs. Given the small dataset and the exploratory nature of this study, a single hold-out split with repeated random initialization was preferred over k-fold cross-validation to avoid further reducing the training set size.

2.3 Neural Network Architecture and Hyperparameter Search

A Multilayer Perceptron (MLP) was implemented in MATLAB R2021B. The architecture consisted of an input layer (12 neurons), a single hidden layer with a variable number of neurons, and a linear output layer (6 neurons). A systematic search was conducted over two key hyperparameters:

- Number of Hidden Neurons: $\{10, 12, 14, 16, 18\}$
- Training Algorithm: Levenberg–Marquardt and Scaled Conjugate Gradient

The hyperbolic tangent (tanh) activation function was used in the hidden layer. Weights were initialized randomly. Training was stopped if the gradient fell below 10^{-6}, 1000 epochs were reached, or the validation error increased for 6 consecutive epochs (early stopping).

2.4 Performance Metrics and Model Selection Criteria

Model performance was evaluated using a two-tiered approach:

- **Primary (Regression):** The core task is multi-output regression. Performance was assessed on the test set using Mean Squared Error (MSE), Root MSE (RMSE), and the coefficient of determination (R^2). The correlation between actual and predicted values (R) was also calculated.

- **Secondary (Clinical Interpretation):** To facilitate clinical understanding, continuous predictions were discretized into 'Low' and 'High' categories. The threshold for each output variable was defined based on the clinical interpretation ranges established by the PM specialist and the distribution of the training data (For instance, for Warmness #1, scores ≤ 2 were categorized as 'Low' and scores > 2 as 'High', based on the PM specialist's clinical reference ranges). Accuracy, Sensitivity, and Specificity were then computed from these dichotomized outcomes.

Model selection was based on:

- Lowest Test MSE as the primary criterion.
- Highest Test R^2 / Correlation as a secondary criterion.
- Stability (low standard deviation across runs).
- Parsimony (fewer neurons preferred if performance was comparable).

2.5 Mathematical Formulation of the Model and Optimization Algorithms

2.5.1 Artificial Neural Network Architecture

The implemented Multilayer Perceptron (MLP) performs a nonlinear mapping $f : \mathbb{R}^{12} \to \mathbb{R}^6$ from the input features (pulse parameters and gender) to the output variables (temperamental qualities and strength). For a network with one hidden layer containing H neurons, the forward propagation for a single input vector $\mathbf{x}$ is defined as follows (Choi , 2025; Menhaj , 2008):

Hidden Layer Output:

The net input z_j and activation a_j of the j-th hidden neuron ($j = 1, \ldots, H$) are computed as:

$$z_j = \sum_{i=1}^{12} w_{ji}^{(1)} x_i + b_j^{(1)}, \quad a_j = \phi\left(z_j\right) = \tanh\left(z_j\right) \qquad (1)$$

where $w_{ji}^{(1)}$ is the weight from input i to hidden neuron j, $b_j^{(1)}$ is the bias term, and $\phi(\cdot)$ denotes the hyperbolic tangent activation function.

Output Layer:

The k-th output neuron ($k = 1, \ldots, 6$) computes:

$$\widehat{y}_k = \sum_{j=1}^{H} w_{kj}^{(2)} a_j + b_k^{(2)} \qquad (2)$$

where $w_{kj}^{(2)}$ and $b_k^{(2)}$ are the output layer weights and bias, respectively. A linear activation function is applied in the output layer.

The complete set of network parameters is denoted as $\Theta = \{\mathbf{W}^{(1)}, \mathbf{b}^{(1)}, \mathbf{W}^{(2)}, \mathbf{b}^{(2)}\}$.

The learning objective is to minimize the discrepancy between the network predictions $\widehat{\mathbf{y}}$ and the true target values $\mathbf{y}$.

2.5.2 Training Objective

The primary objective is to minimize the Mean Squared Error (MSE) over the training dataset of size N_{train} (Ramón-Fernández et al. , 2020):

$$\mathcal{L}(\Theta) = \frac{1}{N_{\text{train}}} \sum_{n=1}^{N_{\text{train}}} \sum_{k=1}^{6} \left(y_k^{(n)} - \widehat{y}_k^{(n)}(\Theta) \right)^2 \qquad (3)$$

2.5.3 Optimization Algorithms

Two second-order optimization algorithms were systematically compared to minimize $\mathcal{L}(\Theta)$: the **Scaled Conjugate Gradient (SCG)** and the **Levenberg–Marquardt (LM)** algorithm (Ramón-Fernández et al. , 2020; Li et al. , 2025).

A. Scaled Conjugate Gradient (SCG) Algorithm

SCG is a conjugate gradient method adapted for supervised learning in neural networks. It avoids the computationally expensive line search of standard conjugate gradient methods by using a trust region approach to scale the step size. The parameter update at iteration t is given by:

$$\Theta^{(t+1)} = \Theta^{(t)} + \alpha^{(t)} \mathbf{p}^{(t)} \qquad (4)$$

where $\mathbf{p}^{(t)}$ is the conjugate direction vector and $\alpha^{(t)}$ is the step size determined from a quadratic approximation within a trust region, ensuring sufficient decrease in error. This approach is memory-efficient and suitable for problems with a large number of parameters.

B. Levenberg–Marquardt (LM) Algorithm

The LM algorithm is a robust approximation to Newton's method designed for minimizing sum-of-squares error functions such as MSE. At each iteration, the parameter update δ is obtained by solving:

$$\left(\mathbf{J}^T\mathbf{J} + \lambda\mathbf{I}\right)\delta = -\mathbf{J}^T\mathbf{e} \qquad (5)$$

where:

- $\mathbf{J}$ is the Jacobian matrix containing the first derivatives of the network errors with respect to Θ,
- $\mathbf{e}$ is the vector of errors $(\mathbf{y} - \widehat{\mathbf{y}})$ for all samples and outputs,
- λ is an adaptive damping factor, and
- $\mathbf{I}$ is the identity matrix.

The algorithm interpolates between gradient descent (for large λ) and the Gauss–Newton method (for small λ). While LM converges rapidly for medium-sized problems, it requires the computation and inversion of $\mathbf{J}^T\mathbf{J}$, which can be memory-intensive for large networks.

2.5.4 Formal Definition of Performance Metrics

Regression Metrics (Li et al. , 2025):

Mean Squared Error (MSE):

$$\mathrm{MSE}_{\mathrm{test}} = \frac{1}{N_{\mathrm{test}}} \sum_{n=1}^{N_{\mathrm{test}}} \sum_{k=1}^{6} \left(y_k^{(n)} - \widehat{y}_k^{(n)}\right)^2 \qquad (6)$$

Coefficient of Determination (R^2):

$$R^2 = 1 - \frac{\sum_{n=1}^{N_{\mathrm{test}}} \sum_{k=1}^{6} \left(y_k^{(n)} - \widehat{y}_k^{(n)}\right)^2}{\sum_{n=1}^{N_{\mathrm{test}}} \sum_{k=1}^{6} \left(y_k^{(n)} - \bar{y}_k\right)^2} \qquad (7)$$

where $\bar{y}_k$ is the mean of the true values for output k.

Classification Metrics (from Dichotomized Outputs):

Performance was evaluated via a confusion matrix for each binarized output, yielding (Barnova et al. , 2026):

$$\mathrm{Accuracy} = \frac{TP + TN}{TP + TN + FP + FN} \qquad (8)$$

$$\mathrm{Sensitivity} = \frac{TP}{TP + FN} \qquad (9)$$

$$\text{Specificity} = \frac{TN}{TN + FP} \qquad (10)$$

where TP, TN, FP, FN denote True Positives, True Negatives, False Positives, and False Negatives, respectively.

2.6 Model Interpretation and Statistical Analysis

A sensitivity analysis was performed on the final selected model to determine feature importance. Each input variable was perturbed by ±10%, and the average absolute change in each output was recorded. This quantifies the relative influence of each pulse parameter and gender on the predictions. Statistical analyses and visualizations were generated using MATLAB R2021b.

2.7 Reproducibility

All random number generator seeds were fixed for data splitting and weight initialization to ensure complete reproducibility. The anonymized dataset and analysis scripts are available upon reasonable request.

3. Results

3.1 Hyperparameter Optimization and Algorithm Comparison

A systematic search was conducted to identify the optimal neural network architecture and training algorithm, as described in detail in Section 2.5. Table 2 shows the performance comparison of ANN architectures trained with Levenberg–Marquardt (LM) and Scaled Conjugate Gradient (SCG) algorithms. Values represent mean ± standard deviation across 10 runs. The best-performing configuration for each metric is highlighted in bold.

The SCG algorithm consistently outperformed LM in terms of final test accuracy and stability, as evidenced by lower standard deviations in MSE. The configuration with 12 hidden neurons trained with SCG emerged as optimal, achieving the highest test accuracy (96.43% ± 2.38%) and the lowest mean squared error (96.43% ± 2.38%) with minimal variance, indicating robust generalization.

3.2 Final Model Performance and Regression Analysis

The selected model (SCG, 12 hidden neurons) demonstrated strong predictive capability across all six output variables. The overall correlation between predicted

Table 2: Results of ANN outputs for Scaled Conjugate Gradient (SCG) and Levenberg–Marquardt (LM) algorithms (MSE: Mean squared error).

Algorithm	n	R^2 (Train)	MSE (Test)	MSE Std	Accuracy (Test)
SCG	10	0.923 ± 0.008	0.020 ± 0.010	0.010	$94.84\% \pm 3.64$
SCG	**12**	$\mathbf{0.942 \pm 0.007}$	$\mathbf{0.014 \pm 0.002}$	0.002	$\mathbf{96.43\% \pm 2.38}$
SCG	14	0.939 ± 0.006	0.016 ± 0.005	0.005	$94.84\% \pm 3.44$
SCG	16	0.932 ± 0.008	0.017 ± 0.004	0.004	$94.44\% \pm 1.82$
SCG	18	0.884 ± 0.007	0.029 ± 0.021	0.021	$93.25\% \pm 2.48$
LM	10	0.423 ± 0.008	7.472 ± 12.359	12.359	$87.30\% \pm 4.96$
LM	12	0.621 ± 0.007	0.192 ± 0.168	0.168	$90.87\% \pm 6.56$
LM	**14**	$\mathbf{0.910 \pm 0.007}$	$\mathbf{0.023 \pm 0.019}$	0.019	$93.25\% \pm 4.81$
LM	16	0.904 ± 0.006	0.025 ± 0.010	0.010	$94.05\% \pm 3.15$
LM	18	0.917 ± 0.007	0.020 ± 0.005	0.005	$94.05\% \pm \sim 0$

and actual normalized values on the test set was $R = 0.8428$ (Figure 1), indicating a substantial linear relationship.

3.3 Performance per Output Variable

To facilitate clinical interpretation, the continuous predictions were discretized into "Low" and "High" categories based on established clinical thresholds. The classification performance for each output variable on the test set ($n = 14$) is summarized in Table 3. It should be noted that sensitivity for Coldness could not be calculated due to the absence of positive cases ($n = 0$) in the test set; therefore, only specificity is reported for this variable.

Table 3: Accuracy, sensitivity, and specificity of the designed ANN outputs

Variables	Accuracy	Sensitivity	Specificity
Warmness #1	78.57%	0.333	0.909
Warmness #2	71.43%	0.800	0.667
Coldness	85.71%	-	0.857
Wetness	85.71%	1.000	0.600
Dryness	92.86%	0.500	1.000
Strength	**100.0%**	**1.000**	**1.000**

Cardiac Strength was predicted with perfect accuracy (100%), while the temperamental qualities showed varying performance, with Dryness (92.86%) and Coldness/Wetness (85.71%) being well-estimated. Warmness variables presented a greater challenge, particularly Warmness #1, where high specificity (0.909) but

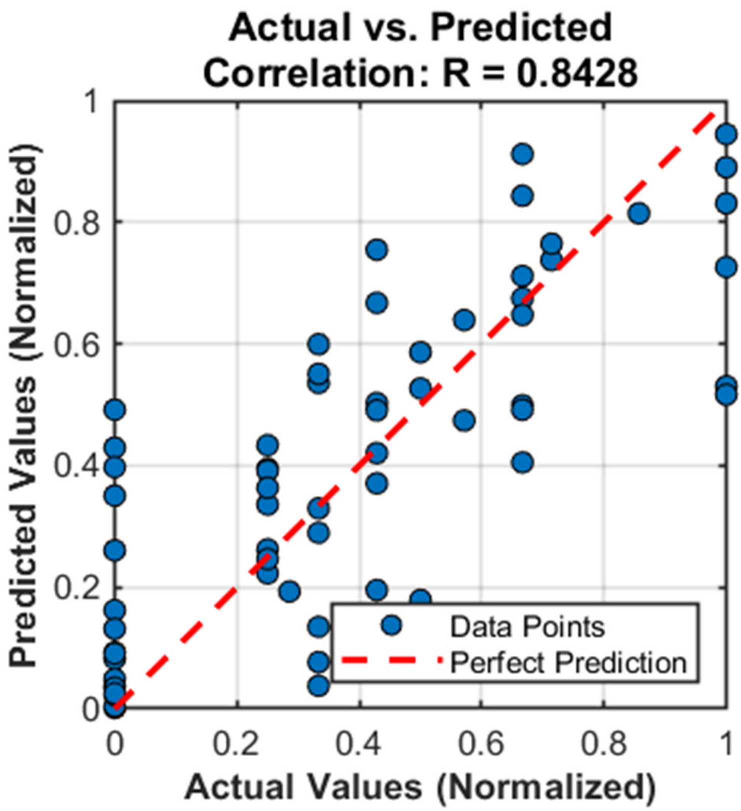

Figure 1: Predicted vs. actual normalized values ($R = 0.8428$; dashed: $y = x$)

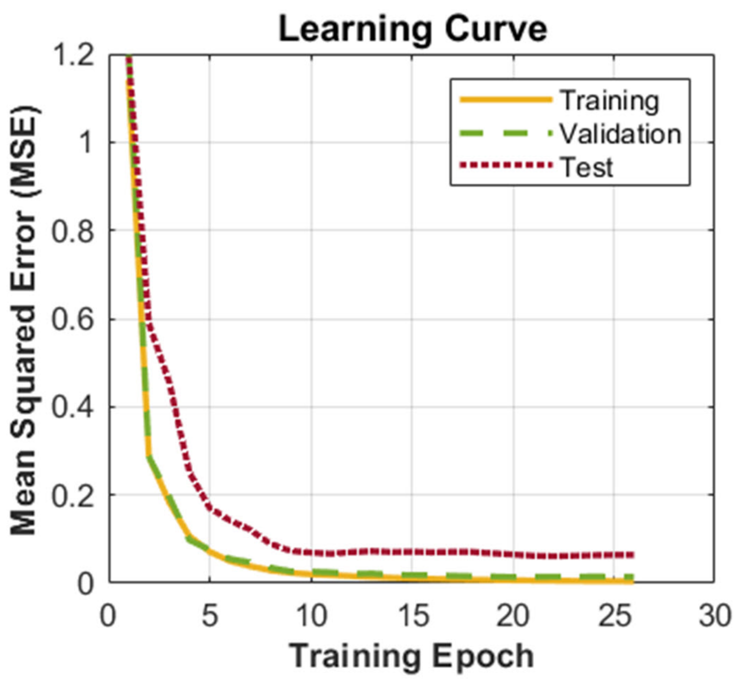

Figure 2: Training, validation, and test MSE vs. epochs; early stopping at epoch 22

lower sensitivity (0.333) indicates a conservative model that rarely misclassifies a truly “Low” individual but may miss some “High” cases.

3.4 Training Dynamics and Convergence

The learning curve for the final model (Figure 2) shows a rapid reduction in error during the initial epochs. The validation error reached its minimum at approximately epoch 22, at which point the early stopping mechanism halted the training to prevent overfitting. This resulted in efficient training, as evidenced by the convergent trajectories of the training, validation, and test errors. The final gradient magnitude was 8.8×10^{-4}, confirming convergence to a flat region of the error surface.

3.5 Feature Importance Analysis

A sensitivity analysis revealed differential importance of input parameters. Pulse Strength (I_3) and Pulse Frequency (I_2) were the most influential parameters for predicting Warmness variables, while thermal measurements (I_9, I_{10}, I_{11}) showed strong contributions to Coldness estimation. The Gender parameter (I_{12}) demonstrated moderate influence across multiple outputs, particularly for Wetness and Dryness predictions, suggesting systematic sex-based differences in pulse manifestations relevant to PM diagnosis.

4. Discussion

This study successfully developed and optimized an artificial neural network (ANN) to estimate the core temperamental qualities and cardiac strength of Persian Medicine (PM) from twelve pulse-derived parameters, including gender. The final model, a Multilayer Perceptron trained with the Scaled Conjugate Gradient (SCG) algorithm and 12 hidden neurons, demonstrated robust performance. It achieved a test set classification accuracy of 96.43% after discretization of outputs, with a strong overall correlation ($R = 0.8428$) between predicted and actual continuous values.

4.1 Algorithm Performance and Model Selection

Contrary to the common preference for the Levenberg–Marquardt (LM) algorithm in medium-sized regression tasks, our systematic comparison revealed the superior efficacy of the SCG algorithm for this specific dataset. The SCG algorithm, particularly with 12 neurons, provided an optimal balance of high accuracy (96.43%), low MSE (0.0139), and minimal performance variance across runs (MSE Std = 0.0023). This finding is consistent with the broader trend in PM computational research, where algorithm performance is highly dependent on data characteristics. For instance, while convolutional neural networks (CNNs) have shown promise for raw signal classification in PM [as demonstrated by Nafisi et al. (2022) for pulse feature extraction] (Nafisi and Ghods , 2022), our results indicate that for tabular, multi-output regression from clinically assessed parameters, a well-tuned MLP with SCG can achieve superior and more stable generalization. The efficient convergence, halted by early stopping at approximately epoch 22, confirms that the model learned the underlying patterns without memorizing noise.

4.2 Clinical Interpretation of Model Outputs

The model's differential performance across the six output variables offers valuable clinical insights. The perfect prediction (100% accuracy, sensitivity, and specificity) of *Cardiac Strength* underscores the strong, direct relationship between objective pulse parameters like strength, speed, and frequency and this PM concept. This aligns with the physiological basis of pulse strength as a marker of myocardial contractility and vascular compliance, a principle explored in both PM and modern cardiovascular studies (Shirbeigi et al. , 2017; Wang et al. , 2021; Huang et al. , 2022). The high accuracy for *Dryness (92.86%)* and *Coldness/Wetness (85.71%)* suggests these qualities are also well-encoded in the pulse profile. The lower sensitivity for *Warmness #1 (33.3%)*, despite high specificity (90.9%), indicates a systematic challenge. This may reflect the inherent complexity of "warmth" as a metabolic composite in PM, which may not have a linear relationship with pulse signs. The better performance on *Warmness #2*, which incorporates intensity scores, suggests that a weighted, continuous approach to quantifying warmth—more akin to the fuzzy logic systems used by Dehghandar et al. (2025) to estimate peripheral resistance from pulse strength and frequency (Dehghandar et al. , 2025)—is more aligned with the ANN's pattern recognition capabilities than a simple count-based method. In practice, the trained ANN could be deployed as a decision support tool within a clinical software interface. A practitioner would input the 12 measured pulse parameters (obtained via standard PM examination), and the model would instantly output estimated scores for warmness, coldness, wetness, dryness, and cardiac strength. This could serve as a second opinion for trainees or as a consistency check for experienced clinicians.

4.3 Feature Importance and Diagnostic Correlates

The sensitivity analysis revealed that *Pulse Strength and Frequency* were primary drivers for predicting warmth-related outputs. This aligns perfectly with classical PM texts (Alizadeh et al. , 2017) and is strongly supported by contemporary computational PM research. For example, Dehghandar et al. (2025) identified pulse strength and frequency as the key parameters for estimating peripheral resistance via a fuzzy system, noting an inverse relationship between strength and resistance (Dehghandar et al. , 2025). Our ANN model independently corroborates the diagnostic primacy of these two parameters, demonstrating their broad utility across different computational frameworks (fuzzy systems vs. ANNs) and target outcomes (peripheral resistance vs. temperamental warmth). The significant contribution of *gender* to predictions of Wetness and Dryness provides quantitative support for longstanding PM observations regarding constitutional differences between sexes (Shirbeigi et al. , 2017; Vaghasloo , 2013). This finding suggests that gender should be an integral, rather than incidental, factor in automated pulse diagnosis systems to improve biological accuracy and personalization. Furthermore, the model identified *thermal parameters* as key contributors to the estimation of Coldness. This validates the classical PM emphasis on local temperature as a sign of metabolic state (Alizadeh et al. , 2017) and is supported by modern studies linking peripheral skin temperature to cardiovascular function (Wang et al. , 2021; Yang et al. , 2021; Quanyu , 2022).

4.4 Comparative Analysis and Advancing PM Diagnostics

This study advances the field of computational PM by moving beyond single-parameter estimation or device-focused signal classification. While Nafisi et al. (2022) used CNNs to classify discrete pulse characteristics from a custom device (Nafisi and Ghods , 2022), our work tackles the more complex task of estimating continuous, holistic qualities from expert-assessed parameters. Similarly, Dehghandar et al. (2025) modeled the relationship between two pulse parameters and a single physiological index using a fuzzy system (Dehghandar et al. , 2025), whereas our ANN simultaneously estimates six interrelated PM qualities. These approaches are complementary: fuzzy systems and ANNs offer different balances of interpretability and predictive power for multi-parameter PM diagnostics.

4.5 Limitations and Future Directions

The primary limitation is the modest sample size ($n = 69$). Future work must prioritize multi-center data collection. Furthermore, integrating explainable AI (XAI) techniques would help bridge the gap between the ANN's predictions and clinical reasoning. A promising direction is the development of a hybrid diagnostic framework, combining the interpretable, rule-based reasoning of fuzzy systems with the pattern recognition power of neural networks for a more transparent and accurate end-to-end system.

5. Conclusion

This study demonstrates the substantial potential of artificial neural networks to formalize and quantify the diagnostic principles of Persian Medicine (PM) pulsology within a rigorous computational framework. By translating qualitative clinical expertise into a stable, high-accuracy predictive model, we provide a practical tool capable of enhancing diagnostic consistency, supporting physician training, and enabling reproducible, data-driven research in PM. The proposed model not only confirms the objective basis of key PM concepts—most notably, the central role of pulse strength and frequency—but also reveals the intrinsically complex and nonlinear nature of warmth estimation, which likely reflects deeper physiological interactions beyond simple parametric descriptions.

Importantly, the present approach does not seek to replace traditional clinical reasoning, but rather to complement it by offering a transparent and quantifiable layer of analysis. In this respect, it stands alongside other computational methodologies in PM, such as fuzzy inference systems for modeling specific heuristic relationships and convolutional neural networks for raw signal classification, while uniquely addressing the structured integration of expert-defined pulse features.

Collectively, this work establishes a foundational framework for the development of intelligent, integrative diagnostic systems that preserve the epistemological depth of traditional medicine while benefiting from the precision and scalability of modern computational science. Future research may extend this framework through larger multicenter datasets, hybrid neuro-symbolic models, and longitudinal analyses, ultimately contributing to the modernization and global scientific validation of Persian Medicine. The modest sample size ($n = 69$) limits generalizability; therefore, the present results should be considered preliminary and require validation on larger, multicenter datasets.

Acknowledgements

The authors would like to thank the participants and clinicians involved in this study.

Conflicts of Interest

The authors declare that there is no conflict of interest concerning this work.

Ethical Approval

In this study, after obtaining informed consent for admission at Ahmadieh PM Clinic of Tehran University of Medical Sciences as a research and training clinic, only routine pulse examination data obtained for health benefits were considered in the analysis; in addition, no confidential personal information or interventions were involved, and thus no additional ethical approval was necessary for this work.

Data Availability

The data used to support the findings of this study are available from the corresponding author upon request.

References

Alizadeh, M., Keshavarz, M., Ebadiani, M., Nazem, E., & Isfahani, M. M. (2012). Complexity and rationality of Avicenna's pulsology. *International Journal of Cardiology,* **157**(3), 434–435. https://doi.org/10.1016/j.ijcard.2012.03.168

Alizadeh, M., Naghizadeh, A., & Keshavarz, M. (2017). The concept of pulse. *Traditional and Integrative Medicine,* **2**(2), 54–60.

Alizadeh, M., Gorji, N., Ghods, R., Shirzad, M., Alizadeh Vaghasloo, M., et al. (2025). Major and minor criteria of heart Mizaj (temperament) diagnosis from the perspective of Persian Medicine: An expert panel study. *Shiraz E-Medical Journal,* **26**(5), e150032. https://doi.org/10.5812/semj-150032

Alizadeh, M., Gorji, N., Ghasemi, V., Hong, L. W., & Mojahedi, M. (2025). A review of heart Mizaj indices in Persian medicine along with a look at Chinese medicine. *Traditional and Integrative Medicine,* **10**(2), 168–178.

Baldi, P., Alexos, A., Domingo, I., & Rahmansetayesh, A. (2025). A theory of synaptic neural balance: From local to global order. *Artificial Intelligence,* **346**, 104360. https://doi.org/10.1016/j.artint.2025.104360

Barnova, K., Martinek, R., Horakova, J., Simetka, O., & Vilimkova Kahankova, R. (2026). Electrohysterography in modern obstetrics: Advances in signal processing, machine learning, and clinical applications. *Artificial Intelligence in Medicine,* **171**, 103303. https://doi.org/10.1016/j.artmed.2026.103303

Chashti, M. A. (2008). *Exir-e-Azam [Great elixir]* (Vol. 3). Research Institute for Islamic and Complementary Medicine.

Chierici, A., Lareyre, F., Iannelli, A., Salucki, B., Goffart, S., Guzzi, L., Poggi, E., Delingette, H., & Raffort, J. (2025). Applications of artificial intelligence in liver cancer: A scoping review. *Artificial Intelligence in Medicine,* **169**, 103241. https://doi.org/10.1016/j.artmed.2025.103241

Choi, S.-M. (2025). Air quality prediction affected by different activation functions and hidden layer nodes in artificial neural network models. *Applied Sciences,* **15**(24), 12863. https://doi.org/10.3390/app152412863

Dehghandar, M. (2016). *Investigating the effect of pulse traditional medicine on the factors of blood pressure by fuzzy calculations* [Master's thesis, Payame Noor University].

Dehghandar, M., Khaloozadeh, H., Soltanian, F., & Keshavarz, M. (2016). Modeling of the pulse parameters in Iranian traditional medicine and estimation of blood pressure by artificial neural network. *Journal of Industrial Engineering Research,* **2**(1), 17–22.

Dehghandar, M., Mirhosseini-Alizamini, M., Alizadeh Vaghasloo, M., & Khosravi Najaf Abadi, A. (2024). Design and implementation of a fuzzy intelligent system to estimate the photoplethysmogram systolic features by Persian medicine pulsology. *Health Management and Information Science,* **10**(4), 226–234. https://doi.org/10.30476/JHMI.2024.102270.1061

Dehghandar, M., Nikbakht, M., & Yousefi Nadar Abadi, F. (2025). Designing a fuzzy stable system to estimate peripheral resistance using frequency and pulse strength parameters of Persian medicine. *Journal of Health and Biomedical Informatics,* **11**(4), 291–305.

Dehghandar, M., Nikbakht, M., & Yousefi, F. (2026). Comparative evaluation of Mamdani and Takagi-Sugeno fuzzy systems for predicting peripheral vascular resistance from photoplethysmogram signals using Persian medicine pulsology. *Digital Chinese Medicine,* **9**(2), 257–264. https://doi.org/10.1016/j.dcmed.2026.05.008

Huang, C., Chen, Y., Li, B., Zhang, Q., Jiang, L., Nie, B., Chen, L., Jian, H., & Xu, G. (2022). Traditional Chinese medicine constitution discrimination model based on metabolomics and random forest decision tree algorithm. *Evidence-Based Complementary and Alternative Medicine,* **2022**, 3490130. https://doi.org/10.1155/2022/3490130

Li, C., Wang, P., Zhou, J., & Mei, X. (2025). Dual intelligent prediction of strength and energy absorption performance of rubber-modified concrete via machine learning and metaheuristic optimization algorithms. *Applied Sciences,* **15**(21), 11680. https://doi.org/10.3390/app152111680

Mellina Andreu, J. L., Bernal, L., Skarmeta, A. F., Ryten, M., Álvarez, S., Cisterna García, A., & Botía, J. A. (2025). PhenoLinker: Phenotype-gene link prediction and explanation using heterogeneous graph neural networks. *Artificial Intelligence in Medicine,* **167**, 103177. https://doi.org/10.1016/j.artmed.2025.103177

Menhaj, M. B. (2008). *Computational intelligence, fundamentals of neural network* (2nd ed.). Amir Kabir University Press.

Mouazen, B., Bendaouia, A., Abdelwahed, E. H., & De Marco, G. (2025). Machine learning and clinical EEG data for multiple sclerosis: A systematic review. *Artificial Intelligence in Medicine,* **166**, 103116. https://doi.org/10.1016/j.artmed.2025.103116

Nafisi, V. (2017). Design and construction of a device for pulse signal analysis and its validity and validity compared to Iranian traditional medicine. *Journal of Traditional Medicine of Islam and Iran,* **8**(1), 1–12.

Nafisi, V. R., & Ghods, R. (2022). A novel pulse-taking device for Persian medicine based on convolutional neural networks. *Journal of Medical Signals & Sensors,* **12**(4), 285–293. https://doi.org/10.4103/jmss.jmss_133_21

Naseri, M., Rezai Zadeh, H., & Choopani, R. (2010). *General overview of traditional medicine.* Nashre Shahr.

Pirooz, F., Ghods, R., & Saberi Isfeedvajani, M. (2026). Agreement between clinical judgment and standardized questionnaires in temperament (Mizaj) assessment in Persian Medicine. *Shiraz E-Medical Journal,* **27**(4), e168654. https://doi.org/10.5812/semj-168654

Quanyu, E. (2022). Pulse signal analysis based on deep learning network. *BioMed Research International,* **2022**, 6256126. https://doi.org/10.1155/2022/6256126

de Ramón-Fernández, A., Salar-García, M. J., Ruiz Fernández, D., Greenman, J., & Ieropoulos, I. A. (2020). Evaluation of artificial neural network algorithms for predicting the effect of the urine flow rate on the power performance of microbial fuel cells. *Energy,* **213**, 118806. https://doi.org/10.1016/j.energy.2020.118806

Rezadoost, H., Karimi, M., & Jafari, M. (2016). Proteomics of hot-wet and cold-dry temperaments proposed in Iranian traditional medicine: A network-based study. *Scientific Reports,* **6**, 30133. https://doi.org/10.1038/srep30133

Rezaeizadeh, H., Alizadeh, M., Naseri, M., & Shams-Ardakani, M. R. (2009). The traditional Iranian medicine point of view on health and disease. *Iranian Journal of Public Health,* **38**(Suppl 1), 169–172.

Sharifi Darani, N., Zargaran, A., Cooper, G. M., Abbassian, A., & Alizadeh Vaghasloo, M. (2021). Hakim Mohammad Azam Khan Chishti (1814–1902) and his book about "Crisis in Diseases". *Traditional and Integrative Medicine,* **6**(2), 166–173.

Shirbeigi, L., Zarei, A., Naghizadeh, A., & Alizadeh Vaghasloo, M. (2017). The concept of temperaments in traditional Persian medicine. *Traditional and Integrative Medicine,* **2**(3), 143–156.

Alizadeh Vaghasloo, M. (2013). *Explaining the ten parameters of pulse diagnosis in traditional Iranian medicine* [Doctoral dissertation, Tehran University of Medical Sciences].

Wang, T., Jin, W., Liang, F., & Alastruey, J. (2021). Machine learning-based pulse wave analysis for early detection of abdominal aortic aneurysms using in silico pulse waves. *Symmetry,* **13**(5), 804. https://doi.org/10.3390/sym13050804

World Health Organization. (2014). *WHO traditional medicine strategy: 2014–2023*. https://www.who.int/publications/i/item/9789241506096

Yang, J., Yang, L., Liu, W., Du, S., Xu, L., He, G., et al. (2021). Analysis of the radial pulse wave and its clinical applications: A survey. *IEEE Access,* **9**, 157940–157959. https://doi.org/10.1109/ACCESS.2021.3128619